

RESEARCH

FRAMEWORK MATERIALS

Fast growth of single-crystal covalent organic frameworks for laboratory x-ray diffraction

Jing Han¹, Jie Feng¹, Jia Kang¹, Jie-Min Chen¹, Xin-Yu Du¹, San-Yuan Ding¹, Lin Liang^{1,2*}, Wei Wang^{1*}

The imine-exchange strategy makes single-crystal growth of covalent organic frameworks (COFs) with large size (>15 microns) possible but is a time-consuming process (15 to 80 days) that has had limited success (six examples) and restricts structural characterization to synchrotron-radiation sources for x-ray diffraction studies. We developed a $\text{CF}_3\text{COOH}/\text{CF}_3\text{CH}_2\text{NH}_2$ protocol to harvest single-crystal COFs within 1 to 2 days with crystal sizes of up to 150 microns. The generality was exemplified by the feasible growth of 16 high-quality single-crystal COFs that were structurally determined by laboratory single-crystal x-ray diffraction with resolutions of up to 0.79 angstroms. The structures obtained included uncommon interpenetration of networks, and the details of the structural evolution of conformational isomers and host-guest interaction could be determined at the atomic level.

Covalent organic frameworks (COFs) are extended porous crystals formed by the reaction of organic precursors as building blocks, which form two-dimensional (2D) or 3D arrays (1–10). Under typical conditions, the reaction products are small crystallites (powders). The growth of high-quality COF single crystals (11–22) must avoid misassembly of the building blocks. Specifically, the growth of large-sized (>15- μm) single-crystal COFs amenable for x-ray diffraction (XRD) analysis usually requires slow crystallization (at least 15 days) (13). In our previous studies, to construct imine-linked single-crystal COFs from covalent polymerization of amines and aldehydes (13, 16), we employed acetic acid (CH_3COOH) as the catalyst and aniline ($\text{C}_6\text{H}_5\text{NH}_2$) as the modulator. The use of aniline has efficiently converted COF crystallization from imine formation to imine-exchange reactions (Fig. 1A). This approach yielded single-crystal COFs suitable for XRD studies with sizes of 15 to 100 μm but required growth times of 15 to 80 days.

In this study, we report the fast synthesis of large-sized single-crystal COFs. In the presence of 2,2,2-trifluoroacetic acid (CF_3COOH) as the catalyst and 2,2,2-trifluoroethylamine ($\text{CF}_3\text{CH}_2\text{NH}_2$) as the modulator, 16 different COFs with crystal sizes ranging from 50 to 150 μm were synthesized in 1 to 2 days (Fig. 1B). The quality of these single crystals was enough for their single-crystal structures to be directly determined by laboratory XRD with resolutions up to 0.79 Å. These high-resolution XRD data revealed the indeterminate topology, conformational evolution, host-guest interaction,

and dynamic nature of COFs at the atomic level.

Fast synthesis of known COF single crystals

Initially, we replaced CH_3COOH , which has the negative logarithm of the acid dissociation constant (pK_a) of 4.76 (23), with a stronger acid, CF_3COOH , which has a pK_a of 0.23 (23). This change accelerated the imine-exchange process (24–26) for the fast growth of single-crystal COF-300 from the condensation of benzene-1,4-dicarboxaldehyde (BDA, 12 mg, 0.089 mmol) and tetrakis(4-aminophenyl)methane (TAM, 20 mg, 0.052 mmol) in 1,4-dioxane (Fig. 2A) (4). When we used CF_3COOH (6 M, 0.1 ml) as the catalyst and $\text{C}_6\text{H}_5\text{NH}_2$ (81 μl , 10 equiv.) as the modulator, COF-300 was rapidly crystallized as uniform rodlike crystals with the average size of 10 μm in 2 hours (Fig. 2D and scheme S1). However, the crystal size could not be further increased by prolonging the reaction time because $\text{C}_6\text{H}_5\text{NH}_2$ (pK_a $\text{C}_6\text{H}_5\text{NH}_3^+ = 4.62$) (23) was not a suitable nucleation inhibitor when CH_3COOH was replaced by CF_3COOH as a more acidic catalyst (table S1).

Accordingly, we screened a series of organic bases as the compatible modulator (table S2) and optimized the concentration ratios of the acid and the modulator (table S3). We found that, in the presence of CF_3COOH (6 M, 0.1 ml) as the catalyst and $\text{CF}_3\text{CH}_2\text{NH}_2$ (pK_a $\text{CF}_3\text{CH}_2\text{NH}_3^+ = 5.66$, 70 μl , 10 equiv.) (23) as the modulator, single-crystal COF-300 could be harvested within 2 days (Fig. 2A and scheme S2) with the uniform size of 60 μm by 30 μm by 30 μm (Fig. 1B and Fig. 2E). The growth rate of single-crystal COF-300 reached 1.25 $\mu\text{m}/\text{hour}$, which is 21 times as fast as the rate of 0.06 $\mu\text{m}/\text{hour}$ previously reported (Fig. 2C). Using a laboratory single-crystal x-ray diffractometer, we could detect the nascent COF-300 and the hydrated COF-300 ($\text{COF-300-H}_2\text{O}$), and the single-crystal structures could be directly solved as sevenfold-interpenetrated *dia-c7* topology (13, 27) and anisotropically refined with resolutions of 0.83 and 0.81 Å (tables S4 and S5), respectively.

Using the $\text{CF}_3\text{COOH}/\text{CF}_3\text{CH}_2\text{NH}_2$ protocol, we successfully synthesized the previously reported single-crystal COFs (13, 16)—LZU-111, LZU-79, COF-303, and LZU-306—as high-quality single crystals within 2 days (Fig. 1B and schemes S3 to S6). The sizes of LZU-111 (~50 μm) and LZU-79 (~100 μm) obtained were comparable to those achieved previously but required 25 to 40 days for synthesis. The sizes of COF-303 (~100 μm) and LZU-306 (~150 μm) were larger than those previously reported (~15 μm in 15 days for COF-303 and ~50 μm in 25 days for LZU-306).

Taking the noninterpenetrated *pts*-structured LZU-306 (Fig. 2B) as the example, similar to the case of COF-300, the crystallization of LZU-306 occurred rapidly with the $\text{CF}_3\text{COOH}/\text{C}_6\text{H}_5\text{NH}_2$ protocol (Fig. 2F) but resulted in irregular crystals of poor quality. Using the $\text{CF}_3\text{COOH}/\text{CF}_3\text{CH}_2\text{NH}_2$ protocol, after 4 hours, crystallization led to the appearance of uniform microcrystals with the size of ~10 μm that could be observed with optical microscopy. After 12 hours, the crystal size reached ~30 μm (Fig. 2F and fig. S85). After 36 hours, large single crystals (150 μm by 100 μm by 100 μm) had grown (Fig. 2F and fig. S87). The growth rate reached 4.17 $\mu\text{m}/\text{hour}$, which is 52 times as fast as that previously reported for the $\text{CH}_3\text{COOH}/\text{C}_6\text{H}_5\text{NH}_2$ protocol (0.08 $\mu\text{m}/\text{hour}$) (Fig. 2C). We obtained XRD data with a resolution of 1.15 Å with the laboratory light source. The noninterpenetrated single-crystal structure of LZU-306 was directly solved, and all of the nonhydrogen atoms could be anisotropically refined. In the previous work, the resolution for the XRD data reached 1.80 Å (16) with a synchrotron-radiation light source, and the direct determination of the single-crystal structures was unattainable.

We further verified the generality of this $\text{CF}_3\text{COOH}/\text{CF}_3\text{CH}_2\text{NH}_2$ protocol by rapidly growing COF structures as high-quality single crystals. The increase in the growth rate enabled us to optimize the experimental conditions efficiently. As a result, 10 different single-crystal COFs were harvested by simple screening of the suitable solvents and the equivalent of $\text{CF}_3\text{CH}_2\text{NH}_2$ (Fig. 1B, scheme S5, and schemes S8 to S12). The single crystals reached sizes of 60 to 150 μm in 1 to 2 days. Structures from laboratory XRD were directly solved and refined with resolution of up to 0.79 Å (tables S8 to S19). Among these structures, we found an uncommon 3D framework with the complicated fourfold [2+2]-interpenetrated *pts* structure (Fig. 3). We also followed the structural evolution among a series of conformational COF isomers that directly correlated with the subtle changes in the local conformation of the linkages (Fig. 4 and fig. S31). Lastly, we accurately located guest molecules within the pores and further evaluated host-guest interactions in COFs (Fig. 5 and fig. S31).

¹State Key Laboratory of Applied Organic Chemistry, Lanzhou Magnetic Resonance Center, College of Chemistry and Chemical Engineering, Lanzhou University, Lanzhou, Gansu 730000, China. ²Institute of Nanoscience and Nanotechnology, School of Materials and Energy, Lanzhou University, Lanzhou, Gansu 730000, China.

*Corresponding author. Email: wang_wei@lzu.edu.cn (W.W.); lianglin@lzu.edu.cn (L.L.)

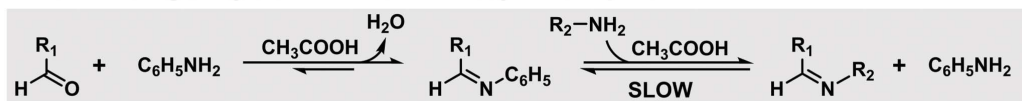
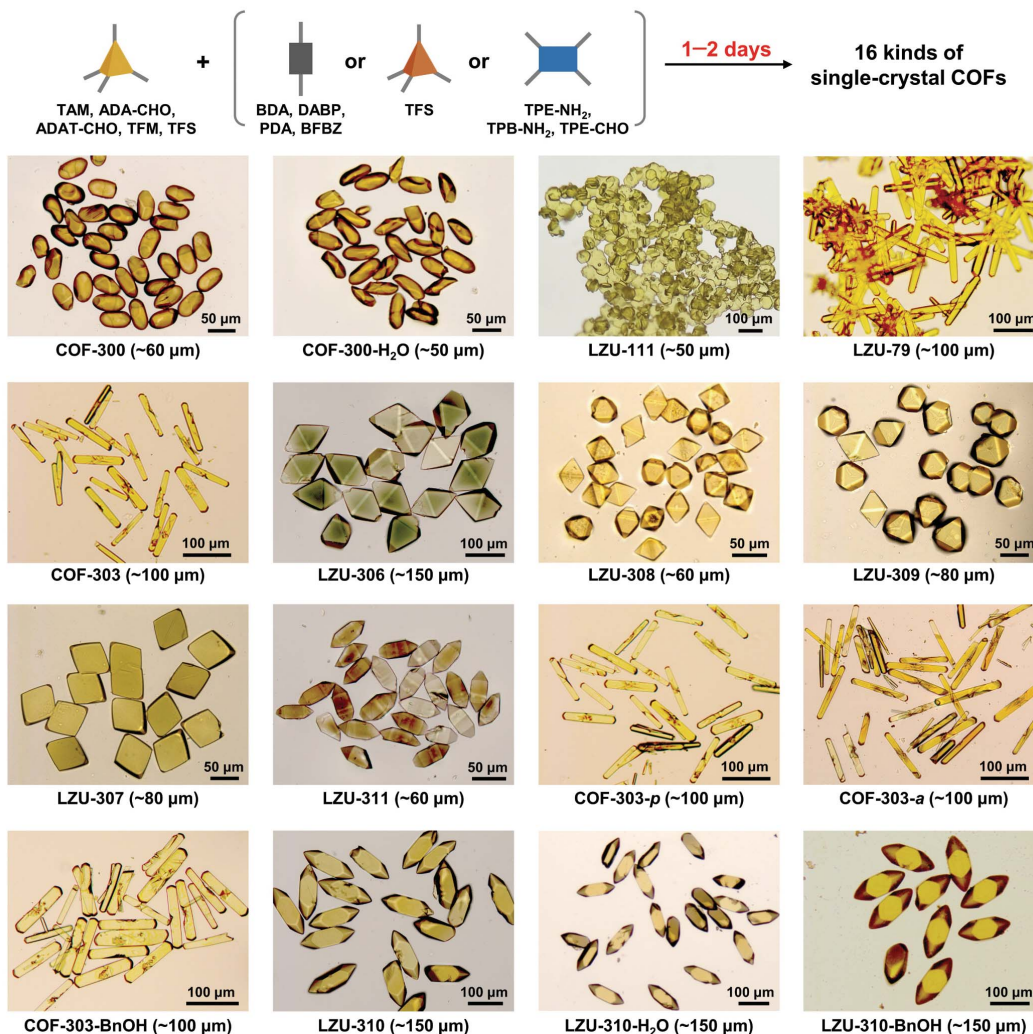
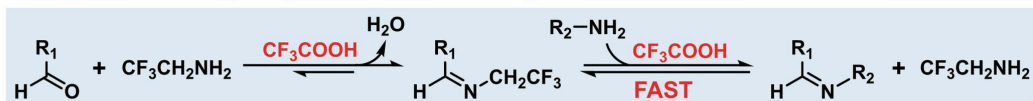
A Growth of single-crystal COFs in 15–80 days in the previous work**B Fast growth of single-crystal COFs in 1–2 days in this work**

Fig. 1. Fast growth of large-sized single-crystal COFs. (A) Imine-exchange strategy that used $\text{CH}_3\text{COOH}/\text{C}_6\text{H}_5\text{NH}_2$ in the previous work for the growth of single-crystal COFs in 15 to 80 days. (B) Protocol developed using $\text{CF}_3\text{COOH}/\text{CF}_3\text{CH}_2\text{NH}_2$ in this work for fast growth of single-crystal COFs in 1 to 2 days. The optical microscopic images for 16 kinds of single-crystal COFs obtained in 1 to 2 days with sizes of 50 to 150 μm are shown. Diversified monomers used in this study for the growth of single-crystal COFs are as follows: TAM,

tetrakis(4-aminophenyl)methane; ADA-CHO, adamantane-1,3,5,7-tetracarbaldehyde; ADAT-CHO, 1,3,5,7-tetrakis(4-formylphenyl)adamantane; TFM, tetrakis(4-formylphenyl)methane; TFS, tetrakis(4-formylphenyl)silane; BDA, benzene-1,4-dicarboxaldehyde; DABP, 4,4'-diaminobiphenyl; PDA, phenylenediamine; BFBZ, 4,7-bis(4-formylbenzyl)-1H-benzimidazole; TPE-NH₂, tetrakis(4-aminophenyl)ethene; TPB-NH₂, 1,2,4,5-tetrakis(4-aminophenyl)benzene; and TPE-CHO, tetrakis(4-formylphenyl)ethene.

Unknown COF structures revealed by $\text{CF}_3\text{COOH}/\text{CF}_3\text{CH}_2\text{NH}_2$ protocol

The $\text{CF}_3\text{COOH}/\text{CF}_3\text{CH}_2\text{NH}_2$ protocol revealed three previously unknown single-crystal COFs with the isorecticular *pts* topology that were

synthesized in 1 day (Fig. 1B and Fig. 3A). LZU-308, constructed from adamantane-1,3,5,7-tetracarbaldehyde (ADA-CHO) and 1,2,4,5-tetrakis(4-aminophenyl)benzene (TPB-NH₂), was crystallized with the size of ~60 μm

in 1 day (scheme S8). LZU-309, formed by TAM and tetrakis(4-formylphenyl)ethene (TPE-CHO), was crystallized with the size reaching ~80 μm in 1 day (scheme S9). LZU-307, produced by 1,3,5,7-tetrakis(4-formylphenyl)

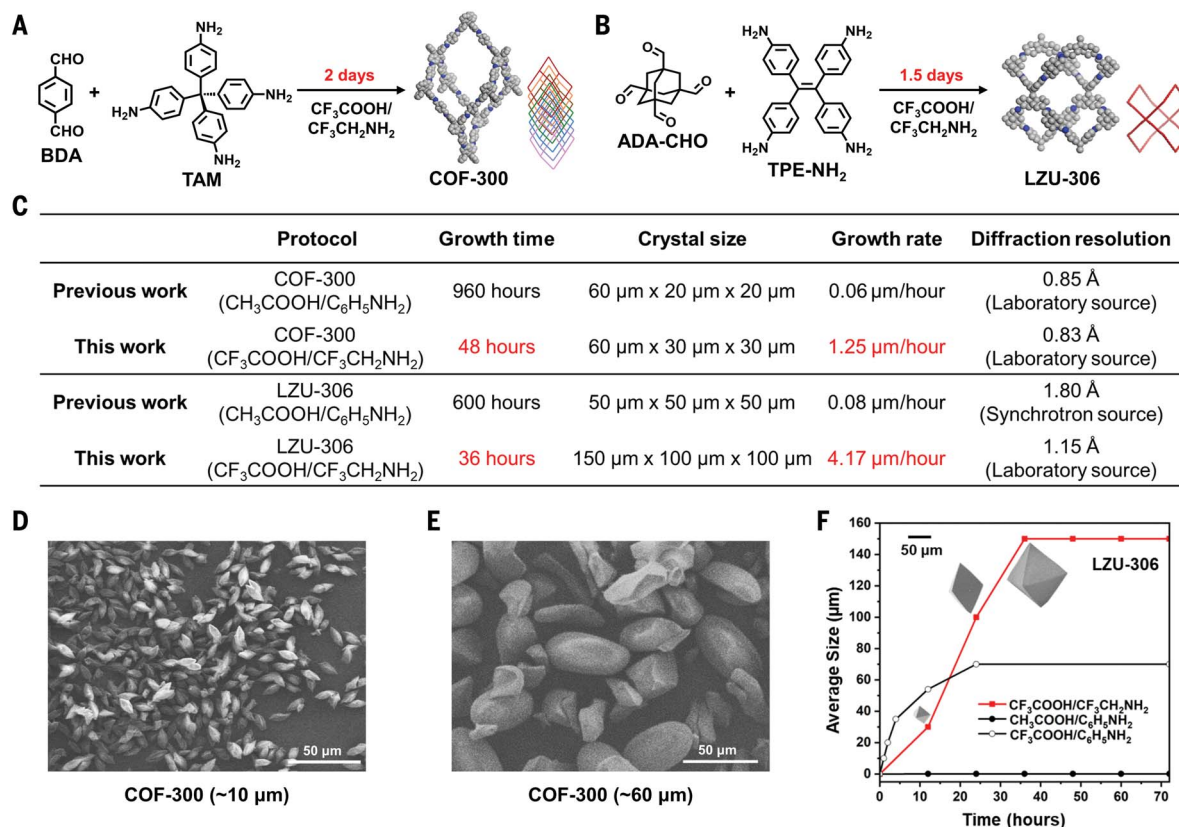


Fig. 2. Fast growth of single-crystal COF-300 and LZU-306. (A and B) Fast growth of single-crystal COF-300 in 2 days and LZU-306 in 1.5 days with the CF₃COOH/CF₃CH₂NH₂ protocol. (C) Comparison of the data for the crystallization time, crystal size, growth rate, and resolution of XRD for COF-300 and LZU-306 reported in the previous work (13, 16) and in this work. (D) The SEM image of

~10 μm-sized COF-300 obtained with the CF₃COOH/C₆H₅NH₂ protocol. (E) The SEM image of ~60 μm-sized COF-300 obtained with the CF₃COOH/CF₃CH₂NH₂ protocol. (F) Average sizes of single-crystal LZU-306 along with the reaction time obtained by using the CF₃COOH/CF₃CH₂NH₂ (red dots, figs. S85 to S87), CH₃COOH/C₆H₅NH₂ (black filled dots), and CF₃COOH/C₆H₅NH₂ (black empty dots, fig. S84) protocols.

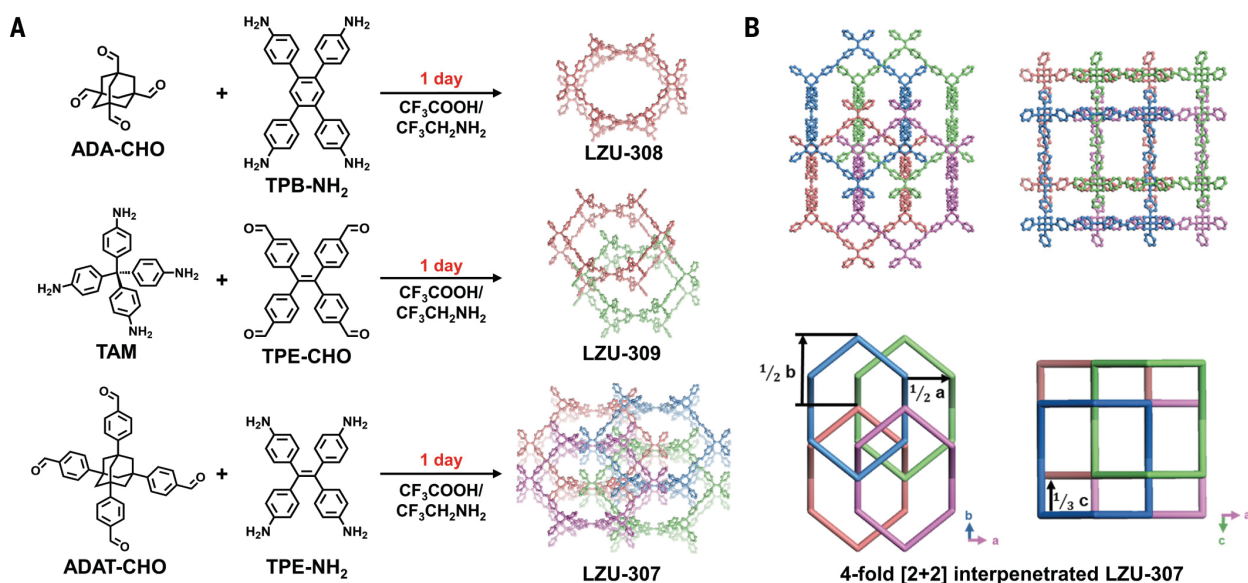


Fig. 3. Fast growth of pts-structured single-crystal LZU-308, LZU-309, and LZU-307 with the CF₃COOH/CF₃CH₂NH₂ protocol. (A) Growth of single crystals of noninterpenetrated LZU-308, twofold-interpenetrated LZU-309, and fourfold [2+2]-interpenetrated LZU-307 in 1 day. (B) Crystal structures and topological structures of LZU-307 viewed along the *c* axis and *b* axis.

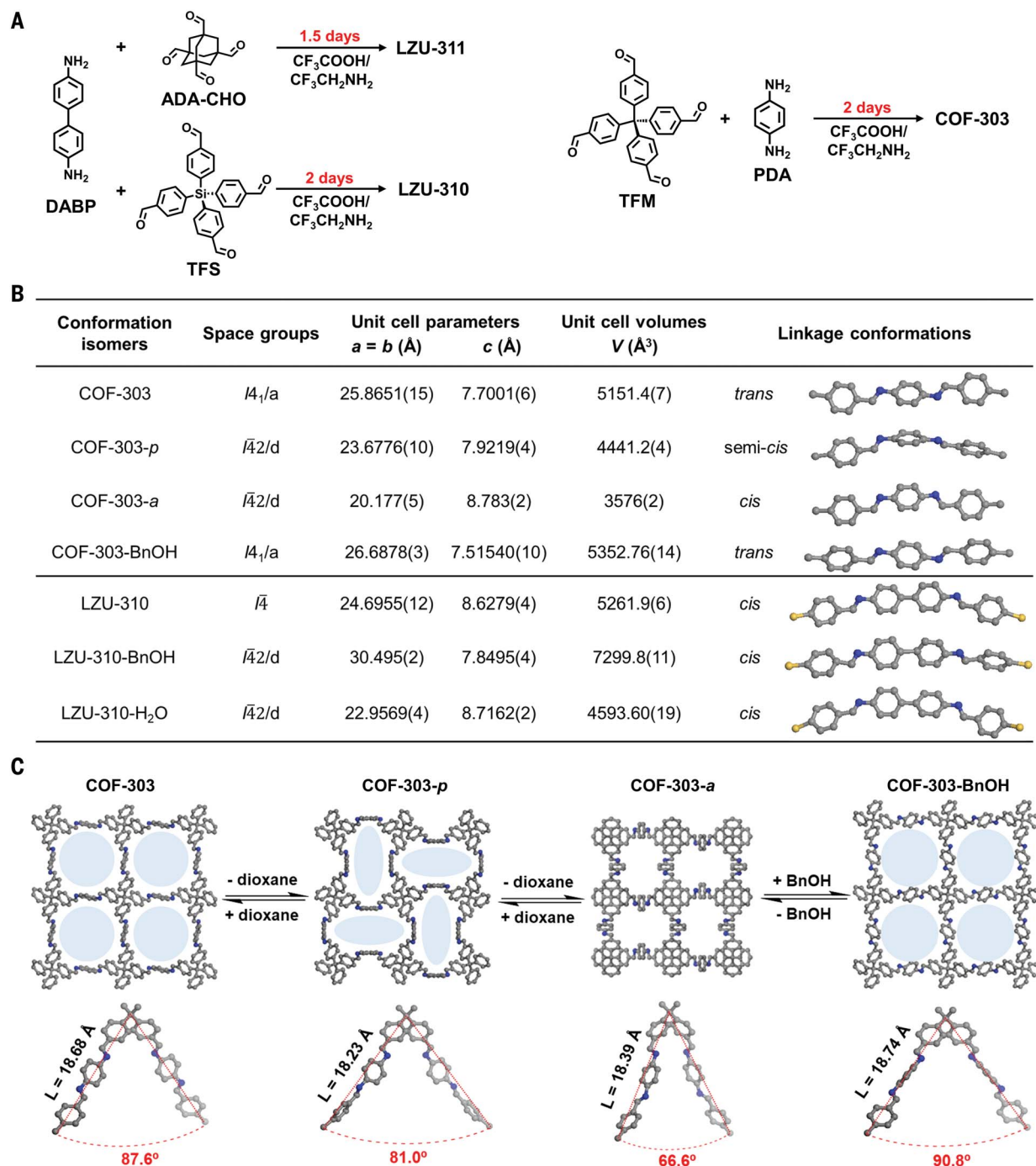


Fig. 4. Synthesis and structural analysis of conformational isomers of single-crystal COFs. (A) Fast growth of single-crystal LZU-311, COF-303, and LZU-310 within 2 days. (B) The space groups, unit-cell parameters, unit-cell volumes, and linkage conformations of the single-crystal isomers. (C) Single-crystal structures and skeleton geometries of COF-303, COF-303-*p*, COF-303-*a*, and COF-303-BnOH. The bottom illustrations show the angle of the tetrahedral node and the length of the linker in each structure.

adamantane (ADAT-CHO) and tetrakis(4-aminophenyl)ethene (TPE-NH₂), was crystallized with the size of ~80 μm in 1 day (scheme S10). We used tetrahydrofuran as the universal solvent for the growth of single-crystal COFs with high quality. Laboratory XRD analysis directly identified the structures of LZU-308,

LZU-309, and LZU-307 as non-, twofold-, and fourfold-interpenetrated *pts* frameworks (Fig. 3A and figs. S10, S12, and S14), respectively. These results served as the experimental evidence that the degree of interpenetration in COFs could be progressively increased with the elongation of the linkers (28). Crystallized with a

rhombohedral morphology, LZU-307 had an uncommon fourfold [2+2]-interpenetrated structure. The space group of LZU-307 was determined as *Cmma*, with unit-cell parameters of $a = 21.947(3)$ Å, $b = 33.671(6)$ Å, and $c = 23.432(3)$ Å (numbers in parenthesis are the error in the last digit) and a large unit-cell volume

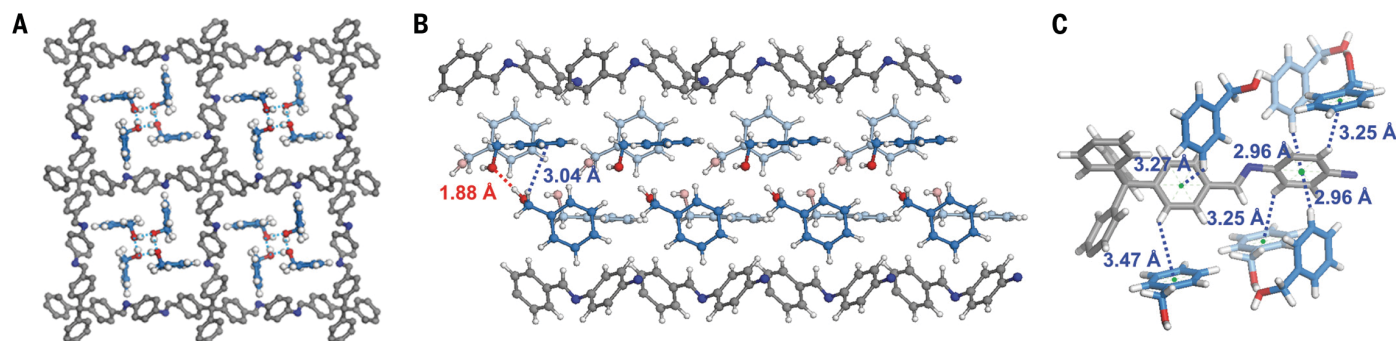


Fig. 5. Host-guest structure of single-crystal COF-303-BnOH. (A) Single-crystal structure of COF-303-BnOH, viewed from the *c* axis. (B) Arrangement of BnOH molecules in the COF-303 channels. The dashed lines in red and blue represent the O-H...O and C-H... π distances between the adjacent BnOH

molecules, respectively. (C) Local structure of COF-303-BnOH, highlighting the C-H... π distances between the COF-303 framework as the host and BnOH as the guest molecule. C atoms of BnOH (light blue); C atoms of COF-303 skeleton (gray); N atoms (blue); O atoms (red); H atoms (white).

of 17316(5) Å³ (table S10). The interpenetration pattern introduced the structural complexity of LZU-307 and led to the low crystallographic symmetry. Specifically, every two of the four independent networks were interlocked with each other along the three different axes through the interpenetration vectors of [0,1/2,1/3], [1/2,0,1/3], and [1/2,1/2,0] (Fig. 3B). The translation vectors along the crystallographic *a* axis (10.97 Å) and *b* axis (16.84 Å) exhibited a common shift of 1/2, while the translation vectors along the *c*-axis (7.81 Å) displayed a distinct shift of 1/3.

The COFs that we synthesized (Fig. 4A) exhibited excellent crystallinity. For example, the laboratory XRD data for LZU-311 (table S11), with a sixfold-interpenetrated *dia* structure, reached a resolution of 0.84 Å. The data for COF-303, COF-303-*p*, COF-303-*a*, and COF-303-BnOH (tables S12 to S15) as sevenfold-interpenetrated conformational isomers reached resolutions of 0.81, 0.79, 0.88, and 0.79 Å, respectively (BnOH, benzyl alcohol); those for LZU-310, LZU-310-H₂O, and LZU-310-BnOH (tables S17 to S19) as ninefold-interpenetrated conformational isomers reached resolutions of 0.81, 0.79, and 0.84 Å, respectively.

Structural transformations and host-guest interactions

The high-resolution XRD data provided key information on the linkage conformation and guest location at the atomic level, through which the structural evolution and dynamic nature of COFs have been clarified. For example, the pores of COF-303 were fully occupied with 1,4-dioxane. The structure was identified as the space group of *I*₄/a with unit-cell parameters of *a* = *b* = 25.8651(15) Å and *c* = 7.7001(6) Å (Fig. 4B and table S12). The adjacent -C=N- and -C=N- linkages exhibited a *trans* conformation. Upon evaporation at 300 K for 10 min, 1,4-dioxane as the guest molecule was partially removed, resulting in the formation of COF-303-*p*. The crystal structure changed to the space group of *I*42*d* with unit-cell parameters of *a* = *b* =

23.6776(10) Å and *c* = 7.9219(4) Å (Fig. 4B and table S13). In this case, the adjacent -C=N- and -C=N- linkages changed to a semi-*cis* conformation.

Upon the complete removal of 1,4-dioxane, the activated COF-303 (COF-303-*a*) underwent an extensive structural transformation in which adjacent linkages were converted to the *cis* form [*a* = *b* = 20.177(5) Å and *c* = 8.783(2) Å] (Fig. 4B and table S14). Analysis on the skeleton geometries indicated that, as the angles of the tetrahedral nodes were decreased from 87.6° (COF-303) to 81.0° (COF-303-*p*) and 66.6° (COF-303-*a*), the unit-cell volumes decreased from 5151.4(7) to 4441.2(4) and 3576(2) Å³ (Fig. 4, B and C), whereas the lengths of the organic linkers remained almost unchanged (from 18.68 to 18.23 and 18.39 Å, Fig. 4C). Further experiments indicated that the structural transformation among these conformational isomers was reversible (table S16 and fig. S46). Thus, the emergence effect (29) exemplified here showed that changes in the global frameworks were governed by subtle but oriented alternation on the conformation of imine linkages.

The laboratory XRD data had sufficient resolution to accurately locate guest molecules within the COF frameworks. For example, COF-303 with BnOH as bulky guests (named COF-303-BnOH) reached an XRD resolution of 0.79 Å that enabled the explicit determination of all of the nonhydrogen atoms in the host-guest structure (table S15). BnOH molecules were arranged into four columns with an interlaced manner through hydrogen bonding (with the O-H...O distance of 1.88 Å, red line) and C-H... π interactions (with the C-H... π distance of 3.04 Å, blue line) (Fig. 5, A and B). In addition, the T-shaped π interaction in the host-guest structure was identified in four types with the C-H... π distances of 2.96, 3.25, 3.27, and 3.47 Å, respectively (Fig. 5C). Compared with the COF-303-*a* structure, COF-303-BnOH was expanded with a 50% increase in the unit-cell volume (Fig. 4, B and C). Accordingly, this dynamic expansion was induced by the aggregation of bulky BnOH guests within the COF-303 channels through the

host-guest interaction that has been demonstrated in Fig. 5.

The conformational transformation triggered by guest molecules was also observed for the ninefold interpenetrated single-crystal COF, LZU-310 (Fig. 4B, fig. S31, and tables S17 to S19). Unlike the case of BnOH as the guest molecule, a dynamic contraction occurred upon the aggregation of water guests within the LZU-310 channels. This contraction was caused by the stronger interaction between water molecules and nitrogen atoms of the LZU-310 framework, as visualized by the shorter distance of 1.99 Å (fig. S31, D and E). Accordingly, the XRD information, with high accuracy, not only rendered single-crystal COFs as candidates for crystalline sponge (30, 31) but also provided in-depth understanding of the structural adaptability and responsiveness of dynamic COFs.

Discussion

It has been acknowledged that the nucleation barrier for crystallization could be reduced by adding catalysts into the system (32, 33). The formation of single-crystal COFs in our work was based on covalent polymerization through imine-exchange reactions that can be effectively catalyzed by acids (25). When CH₃COOH was replaced with the stronger acid, CF₃COOH, the growth rates of single-crystal COFs were significantly enhanced (83 and 57 times for COF-300 and LZU-306, respectively, table S1). Its synergy with CF₃CH₂NH₂ as the compatible modulator ensured the universal harvest of large-sized (50- to 150- μ m) single crystals of 3D COFs with high quality in 1 to 2 days. We further found that the CF₃COOH/CF₃CH₂NH₂ protocol also enabled the growth of a 2D single-crystal COF (34), LZU-115, reaching a size of ~10 μ m within 2 days (scheme S13 and figs. S124 and S125). Accordingly, the fast growth of single-crystal COFs for laboratory XRD analysis would probably renew the research paradigm for precise assembly across the length scale through covalent bonding. This finding challenges the traditional belief

(35) that the growth of high-quality single crystals requires slow crystallization with the cost of time consumption.

During the revision of this manuscript, Yu *et al.* reported the fast growth of a large-sized (up to 450 μm) single-crystal COF within 5 days (36).

REFERENCES AND NOTES

1. A. P. Côté *et al.*, *Science* **310**, 1166–1170 (2005).
2. H. M. El-Kaderi *et al.*, *Science* **316**, 268–272 (2007).
3. C. S. Diercks, O. M. Yaghi, *Science* **355**, eaal1585 (2017).
4. F. J. Uribe-Romo *et al.*, *J. Am. Chem. Soc.* **131**, 4570–4571 (2009).
5. S. Y. Ding *et al.*, *J. Am. Chem. Soc.* **133**, 19816–19822 (2011).
6. S. Kandambeth *et al.*, *J. Am. Chem. Soc.* **134**, 19524–19527 (2012).
7. S.-Y. Ding, W. Wang, *Chem. Soc. Rev.* **42**, 548–568 (2013).
8. E. Jin *et al.*, *Science* **357**, 673–676 (2017).
9. X. Wang *et al.*, *Nat. Chem.* **10**, 1180–1189 (2018).
10. W. Zhang *et al.*, *Nature* **604**, 72–79 (2022).
11. Y.-B. Zhang *et al.*, *J. Am. Chem. Soc.* **135**, 16336–16339 (2013).
12. D. Beaudoin, T. Maris, J. D. Wuest, *Nat. Chem.* **5**, 830–834 (2013).
13. T. Ma *et al.*, *Science* **361**, 48–52 (2018).
14. J. A. R. Navarro, *Science* **361**, 35–35 (2018).
15. A. M. Evans *et al.*, *Science* **361**, 52–57 (2018).
16. L. Liang *et al.*, *Angew. Chem. Int. Ed.* **59**, 17991–17995 (2020).
17. H.-S. Xu *et al.*, *Nat. Commun.* **11**, 1434 (2020).
18. L. Peng *et al.*, *Nat. Commun.* **12**, 5077 (2021).
19. C. Kang *et al.*, *Nat. Commun.* **13**, 1370 (2022).
20. A. Natraj *et al.*, *J. Am. Chem. Soc.* **144**, 19813–19824 (2022).
21. S. Wang *et al.*, *J. Am. Chem. Soc.* **145**, 12155–12163 (2023).
22. Z. Zhou *et al.*, *Nat. Chem.* **15**, 841–847 (2023).
23. J.-D. Yang, X.-S. Xue, P. Ji, X. Li, J.-P. Cheng, Internet Bond-energy Databank (pKa and BDE): iBond Home Page (2024); <http://ibond.nankai.edu.cn>.
24. S. J. Rowan, S. J. Cantrill, G. R. L. Cousins, J. K. M. Sanders, J. F. Stoddart, *Angew. Chem. Int. Ed.* **41**, 898–952 (2002).
25. M. Ciaccia, S. Di Stefano, *Org. Biomol. Chem.* **13**, 646–654 (2015).
26. N. Giuseppone, J.-L. Schmitt, E. Schwartz, J.-M. Lehn, *J. Am. Chem. Soc.* **127**, 5528–5539 (2005).
27. T. Ma *et al.*, *J. Am. Chem. Soc.* **140**, 6763–6766 (2018).
28. H.-L. Jiang, T. A. Makal, H.-C. Zhou, *Coord. Chem. Rev.* **257**, 2232–2249 (2013).
29. P. L. Luisi, *Found. Chem.* **4**, 183–200 (2002).
30. Y. Inokuma *et al.*, *Nature* **495**, 461–466 (2013).
31. S. Lee, E. A. Kapustin, O. M. Yaghi, *Science* **353**, 808–811 (2016).
32. E. Borisenko, Ed., *Crystallization and Materials Science of Modern Artificial and Natural Crystals*, (InTech, 2012), p. 253.
33. L. Li *et al.*, *New J. Chem.* **47**, 20703–20707 (2023).
34. L. Wang, J. Liu, J. Wang, J. Huang, *Chem. Eng. J.* **473**, 145405 (2023).
35. B. R. Pamplin, *Crystal Growth* (Pergamon Press, 1980).
36. B. Yu *et al.*, *Nat. Chem.* **16**, 114–121 (2024).

ACKNOWLEDGMENTS

J.H., L.L., and W.W. thank Y.-L. Shao, H. Wang, and G.-H. Xi for assisting with the XRD data collection and S. Chen and S. Guo for assisting with CO₂ adsorption-desorption experiments. Insightful discussions with T. Ma and W. Yu, Y. Li, O. M. Yaghi, and J.-L. Sun are much appreciated. **Funding:** This work was financially supported by the National Key R&D Program of China (no. 2022YFA1503300), the National Natural Science Foundation of

China (no. 92056202), the China Postdoctoral Science Foundation (no. 2021M691373), and the China Postdoctoral Innovation Talents Support Program (no. BX20211116). **Author contributions:** W.W. led the project. J.F., J.H., L.L., and W.W. conceived the idea. J.H., L.L., J.K., and J.-M.C. conducted the synthesis and crystal growth of 3D COFs. X.-Y.D. conducted the growth of 2D single-crystal COFs. L.L. and J.H. carried out the crystallographic studies. J.H., L.L., J.-M.C., and J.K. carried out the characterizations. J.H., L.L., J.K., and X.-Y.D. took the crystal images and photos. J.H., L.L., J.F., J.-M.C., S.-Y.D., and W.W. discussed the results. L.L., J.H., and W.W. interpreted the results and wrote the manuscript.

Competing interests: The authors declare that they have no competing interests. **Data and materials availability:** Crystallographic data reported in this paper are tabulated in the supplementary materials and archived at the Cambridge Crystallographic Data Centre (CCDC) under reference nos. CCDC 2294453 to 2294464 and 2294641 to 2294643. All other data needed to evaluate the conclusions in the paper are present in the paper or the supplementary materials.

License information: Copyright © 2024 the authors, some rights reserved; exclusive licensee American Association for the Advancement of Science. No claim to original US government works. <https://www.science.org/about/science-licenses-journal-article-reuse>

SUPPLEMENTARY MATERIALS

[science.org/doi/10.1126/science.adk8680](https://doi.org/10.1126/science.adk8680)

Materials and Methods

Supplementary Text

Figs. S1 to S125

Tables S1 to S19

References (37–43)

Data S1 to S27

Checkcif files for Data S1 to S15

Submitted 15 September 2023; accepted 17 January 2024

10.1126/science.adk8680

Erratum

Erratum for the Research Article “Fast growth of single-crystal covalent organic frameworks for laboratory x-ray diffraction” by J. Han *et al.*

During the revision of the Research Article “Fast growth of single-crystal covalent organic frameworks for laboratory x-ray diffraction” (1 March 2024, p. 1014), an independent research group, Yu *et al.*, reported the fast growth of a large-sized (up to 450 μm) single-crystal covalent organic framework within 5 days [B. Yu *et al.*, *Nat. Chem.* **16**, 114 (2024)]. Yu *et al.*’s paper supports the Han *et al.* Research Article’s finding of fast growth of single-crystal covalent organic frameworks. The Yu *et al.* paper has been added as reference 36 to document the additional evidence, and other references have been renumbered accordingly. The reference is cited at the end of a new, final line of text. The Yu *et al.* findings do not change any of Han *et al.*’s conclusions.